plate behavior substantiate those of Ref. 2 which were obtained using a shear deformation theory developed by Ambartsumyan.[1] To the authors' knowledge, this is the only other shear deformation theory developed specifically for applications to laminated plates.

Other numerical results indicate that the criteria for applying thin-plate theory (CPT) to laminated plates is not well defined. For example, for certain laminates, the deformed normal severely warps causing the maximum transverse shear stress to be carried in the facing layers. Limits on the lamina thicknesses, the material types and layer orientations which ensure that this undesirable effect does not occur need to be established.

References

[1] Ambartsumyan, S. A., *Theory of Anisotropic Plates*, translated from Russian by T. Cheron and edited by J. E. Ashton, Technomic Publishing Co., Stamford, 1969.

[2] Whitney, J. M., "The Effect of Transverse Shear Deformation on the Bending of Laminated Plates," *Journal of Composite Materials*, Vol. 3, 1969, p. 534.

[3] Pagano, N. J., "Exact Solutions for Composite Laminates in Cylindrical Bending," *Journal of Composite Materials*, Vol. 3, 1969, p. 398.

[4] Pagano, N. J., "Analysis of the Flexure Test of Bidirectional Composites," *Journal of Composite Materials*, Vol. 1, 1967, p. 336.

[5] Pagano, N. J., "Exact Solutions for Rectangular Bidirectional Composites and Sandwich Plates," *Journal of Composite Materials*, Vol. 4, 1970, p. 20.

[6] Whitney, J. M. and Leissa, A. W., "Analysis of Heterogenous Anisotropic Plates," *Journal of Applied Mechanics*, Vol. 36, 1969, pp. 261–266.

[7] Calcote, L. R., *The Analysis of Laminated Composite Structures*, Van Nostrand-Reinhold, New York, 1969.

[8] Clough, R. W. and Felippa, C. A., "A Refined Quadrilateral Element for Analysis of Plate Bending," *Proceedings II Conference on Matrix Methods in Structural Mechanics*, Wright-Patterson Air Force Base, Ohio, 1968.

[9] Reissner, E., "The Effect of Transverse Shear Deformation on the Bending of Elastic Plates," *Journal of Applied Mechanics*, Vol. 12, 1945, pp. 69–77.

[10] Pryor, C. W., Jr., "Finite Element Analysis of Laminated Anisotropic Plates," Ph. D. dissertation, 1970, Virginia Polytechnic Institute.

MAY 1971 AIAA JOURNAL VOL. 9, NO. 5

Buckling of Stiffened Multilayered Circular Cylindrical Shells with Different Orthotropic Moduli in Tension and Compression

ROBERT M. JONES*

The Aerospace Corporation, San Bernardino, Calif.

An exact buckling criterion, within the framework of classical buckling theory, is derived for eccentrically stiffened multilayered circular cylindrical shells made of materials that have different orthotropic moduli in tension and compression. Such behavior is typical of many current composite materials. The buckling criterion is valid for arbitrary combinations of axial and circumferential loading, including axial compression and internal pressure as well as axial tension and lateral pressure. The material model (stress-strain relationship) involves a bilinear stress-strain curve that has a discontinuity in slope (modulus) at the origin. A numerical example of buckling of a ring-stiffened two-layered circular cylindrical shell is given to illustrate application of the buckling criterion.

Nomenclature†

a = ring spacing (Fig. 3)
A = cross-sectional area of a stiffener
A_{ij} = coefficients in buckling criterion Eq. (30)
b = stringer spacing (Fig. 3)
B_{ij} = extensional stiffnesses of the layered shell
C_{ij} = coupling stiffnesses of the layered shell
D_{ij} = bending stiffnesses of the layered shell
E = Young's modulus of an isotropic material
E_x,E_y = Young's moduli in x and y directions, respectively
E_{45} = Young's modulus at 45° to principal axes of orthotropy
G = shearing modulus, $E/[2(1+\nu)]$, of a stiffener
I = moment of inertia of a stiffener about its centroid
J = torsional constant of a stiffener
k_x,k_y = weighting factors in compliance matrix Eq. (5)
K_{ij} = stiffnesses in stress-strain relations Eq. (7)
L = length of circular cylindrical shell (Fig. 3)
m = number of axial buckle halfwaves
$\delta M_x,\delta M_y,\delta M_{xy},\delta M_{yx}$ = variations in moments per unit length during buckling
n = number of circumferential buckle waves
N = number of layers in multilayered shell
$\delta N_x,\delta N_y,\delta N_{xy}$ = variations in in-plane forces per unit length during buckling
$\bar{N}_x,\bar{N}_y$ = applied axial and circumferential forces per unit length
p = lateral pressure
P = axial load
R = radius to shell reference surface (Fig. 3)
S_{ij} = compliances in strain-stress relations Eq. (2)
t_k = thickness of kth shell layer
$\delta u,\delta v,\delta w$ = variations of axial, circumferential, and radial displacements during buckling from a membrane prebuckled shape
x,y,z = axial, circumferential, and radial coordinates on shell reference surface (Fig. 3)
$\bar{z}$ = distance from stiffener centroid to shell reference surface (Fig. 3), positive when stiffener on outside
$\epsilon_x,\epsilon_y,\gamma_{xy}$ = in-plane axial, circumferential, and shear strains
$\delta\epsilon_x,\delta\epsilon_y,\delta\gamma_{xy}$ = variations in ϵ_x, ϵ_y, and γ_{xy} during buckling

Received August 28, 1970.

* Member of the Technical Staff, Theoretical Mechanics Section; presently Associate Professor of Aerospace Engineering/Mechanical Engineering and Solid Mechanics, Southern Methodist University Institute of Technology, Dallas, Texas. Associate Fellow AIAA.

† A comma indicates partial differentiation with respect to the subscript following the comma. The prefix δ denotes the variation during buckling of the symbol which follows.

$\delta\epsilon_1,\delta\epsilon_2,\delta\epsilon_3$ = variations in reference surface strains during buckling
δ_k = distance from inner surface of layered shell to outer surface of kth layer
Δ = distance from inner surface of layered shell to reference surface
ν_{xy} = Poisson's ratio for contraction in the y direction due to tension in the x direction
$\sigma_x,\sigma_y,\tau_{xy}$ = in-plane axial, circumferential, and shear stresses
$\delta\sigma_x,\delta\sigma_y,\delta\tau_{xy}$ = variations in σ_x, σ_y, and τ_{xy} during buckling
$\delta\chi_1,\delta\chi_2,\delta\chi_3$ = variations in reference surface curvatures during buckling

Superscript

k = kth shell layer

Subscripts

c = compression
k = kth shell layer
r = ring
s = stringer
t = tension

Introduction

COMPOSITE materials are receiving dramatically increasing attention in structural applications because of important weight savings. Such materials are typically a combination of a usually light, weak, and flexible matrix material with a very strong and stiff reinforcing material in the form of fibers or granules. The resulting composite material is light, yet strong and stiff.

One of the important characteristics of composite materials is that they exhibit different moduli or stiffnesses under tensile and compressive loading.[1] This characteristic behavior is shown schematically in the stress-strain curve of Fig. 1. Actual stress-strain behavior is probably not as simple as shown in Fig. 1. Rather, a nonlinear transition region may exist between the essentially linear tensile and compressive portions of the stress-strain curve.[2] The measurement of strains near zero stress is extremely difficult to perform with accuracy. However, the stress-strain behavior may be as shown in Fig. 2, where replacement of the hypothesized actual behavior by a bilinear stress-strain curve is offered as a simplification of the obviously nonlinear behavior. Moreover, for most materials, there is not enough mechanical property data on which to base the more complex model. One possible disadvantage of the bilinear model is that a discontinuity in slope (modulus) occurs at the origin of the stress-strain curve (see Figs. 1 and 2). The effect of the slope discontinuity is discussed in the body of the paper.

The objective of this paper is to derive an analysis for and present results for buckling of circular cylindrical shells (see Fig. 3) with eccentric stiffeners and multiple orthotropic layers that have different moduli in tension and compression. Ambartsumyan and his co-workers presented stress-strain relations for materials with different moduli in tension and compression.[3-7] However, the shear modulus was not defined in principal stress coordinates so a new material model (stress-strain relationship) is displayed and used in the present paper. The new material model is the basis for determining the variations in stresses during buckling. The paper is a combination and extension of concepts developed by the author for circular cylindrical shells 1) with eccentric stiffeners and multiple orthotropic layers[8] and 2) with different isotropic moduli in tension and compression using the Ambartsumyan material model.[9] The principal axes of orthotropy of the layers coincide with the shell coordinate directions. Each layer of the thin multilayered shell is perfectly bonded (i.e., a non-shear-deformable bond) to adjacent layers. Accordingly, the Kirchhoff-Love hypothesis is invoked in consonance with conventional thin shell theory. One-dimensional beam elements are used to represent the eccentric stiffeners in an approximate manner after Block, Card, and Mikulas.[10] Classical buckling theory, by which is implied a membrane prebuckled shape, is used for the particular simply supported edge boundary conditions $\delta N_x = \delta v = \delta w = \delta M_x = 0$. Although coupling between bending and extension is not, of course, accounted for in the membrane prebuckling state, it is accounted for during buckling. Under arbitrary combinations of biaxial loading, the stress state in the layers is statically indeterminate since the layer material properties depend on the stresses. Procedures are developed for treating the indeterminancy. Next, a buckling criterion, derived herein, is applied to determine the buckling load under arbitrary combinations of axial and lateral pressure including axial tension and external pressure as well as axial compression and internal pressure. A numerical example of buckling of a ring-stiffened two-layered shell is given to illustrate application of the theory.

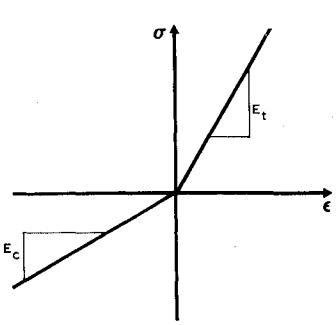

Fig. 1 Stress-strain curve for a material with different moduli in tension and compression.

Derivation of Buckling Criterion

The various moduli in the stress-strain relations for materials with different orthotropic moduli in tension and compression are chosen in the author's material model according to the signs and relative values of the stresses in the indeterminate membrane prebuckling stress state. Thus, the membrane stress state must be determined by searching for the combination of stress signs that is consistent with material properties in each layer that in turn yield the same stress signs. The variations in the biaxial stresses during buckling are then obtained in terms of the variations in strains in each layer of a multilayered circular cylindrical shell during buckling. Subsequently, the variations in biaxial stresses are integrated over the shell layers and the variations in uniaxial stresses are integrated over the stiffeners in order to obtain expressions for the variations in forces and moments during buckling of a stiffened shell. Finally, the variations in forces and moments are substituted in Donnell-type stability differential equations which are solved for a set of simply supported edge boundary conditions. The result is a closed-form buckling criterion in terms of the geometry and material properties of a stiffened multilayered shell. The criterion is applicable for arbitrary combinations of axial and lateral pressure.

Stress-Strain Relations for Orthotropic Materials with Different Moduli in Tension and Compression

For the orthotropic kth layer of a multilayered shell subjected to principal stresses $\sigma_x{}^k$ and $\sigma_y{}^k$ in the shell coordinate directions and having principal axes of orthotropy aligned with the shell coordinate directions, the author's material model can be written as

$$\epsilon_x = S_{11}{}^k\sigma_x{}^k + S_{12}{}^k\sigma_y{}^k \quad (1a)$$

$$\epsilon_y = S_{12}{}^k\sigma_x{}^k + S_{22}{}^k\sigma_y{}^k \quad (1b)$$

The compliances, $S_{ij}{}^k$, are assigned according to

if $\sigma_x{}^k > 0$ and $\sigma_y{}^k > 0$; $S_{ij}{}^k = S_{ij\,t}{}^k$ (2a)

if $\sigma_x^k < 0$ and $\sigma_y^k < 0$; $S_{ij}^k = S_{ijc}^k$ (2b)

if $\sigma_x^k > 0$ and $\sigma_y^k < 0$; $S_{11}^k = S_{11t}^k$

$$S_{12}^k = k_x^k S_{12t}^k + k_y^k S_{12c}^k, \quad S_{22}^k = S_{22c}^k \quad (2c)$$

if $\sigma_x^k < 0$ and $\sigma_y^k > 0$; $S_{11}^k = S_{11c}^k$

$$S_{12}^k = k_x^k S_{12c}^k + k_y^k S_{12t}^k, \quad S_{22}^k = S_{22t}^k \quad (2d)$$

wherein

$$S_{11t}^k = 1/E_{xt}^k, \; S_{12t}^k = -\nu_{xyt}^k/E_{xt}^k, \; S_{22t}^k = 1/E_{yt}^k \quad (3)$$

$$S_{11c}^k = 1/E_{xc}^k, \; S_{12c}^k = -\nu_{xyc}^k/E_{xc}^k, \; S_{22c}^k = 1/E_{yc}^k \quad (4)$$

$$k_x^k = |\sigma_x^k|/(|\sigma_x^k| + |\sigma_y^k|) \quad (5a)$$

$$k_y^k = |\sigma_y^k|/(|\sigma_x^k| + |\sigma_y^k|) \quad (5b)$$

Note that $\nu_{xyt}^k = -\epsilon_y^k/\epsilon_x^k$ for $\sigma_x^k = \sigma$, and all other stresses are zero. The weighting factors k_x^k and k_y^k could be chosen as some other function of the principal stresses. Full qualification of the form of the weighting factors awaits definitive experimental work. By use of the weighting factors, the compliances S_{ij}^k are forced to be symmetric. Since only principal stresses are of concern in this section, discussion of the shearing modulus will be deferred until a later section.

The inverse of the strain-stress relations in Eq. (1) are the stress-strain relations

$$\sigma_x^k = K_{11}^k \epsilon_x^k + K_{12}^k \epsilon_y^k \quad (6a)$$

$$\sigma_y^k = K_{12}^k \epsilon_x^k + K_{22}^k \epsilon_y^k \quad (6b)$$

where

$$K_{11}^k = S_{22}^k/[S_{11}^k S_{22}^k - (S_{12}^k)^2] \quad (7a)$$

$$K_{12}^k = -S_{12}^k/[S_{11}^k S_{22}^k - (S_{12}^k)^2] \quad (7b)$$

$$K_{22}^k = S_{11}^k/[S_{11}^k S_{22}^k - (S_{12}^k)^2] \quad (7c)$$

which for an orthotropic material with the same moduli in tension and compression reduce to

$$K_{11}^k = E_x^k/(1 - \nu_{xy}^k \nu_{yx}^k) \quad (8a)$$

$$K_{12}^k = \nu_{xy}^k E_y^k/(1 - \nu_{xy}^k \nu_{yx}^k) \quad (8b)$$

$$K_{22}^k = E_y^k/(1 - \nu_{xy}^k \nu_{yx}^k) \quad (8c)$$

Determination of Membrane Prebuckling State

In the preceding section, the compliances in the stress-strain relations were given for a single layer of a multilayered shell in terms of the layer stresses. However, the layer stresses cannot be determined from the shell geometry and loading alone; material properties must be known for each layer as well. Thus, in the membrane prebuckling state, both the layer stresses and material properties are indeterminate in a shell with multiple orthotropic layers that have different moduli in tension and compression. Thus, the statically indeterminate prebuckling stress state must be established. This process requires iteration between a chosen set of stress signs and a set of stress signs calculated from the chosen set until the two sets of stress signs agree. In the process, since the cross-compliance S_{12}^k depends on the *magnitude* of the layer stresses, a subiteration must take place to determine the correct S_{12}^k for each chosen set of stress signs. The procedure is described in the following paragraphs.

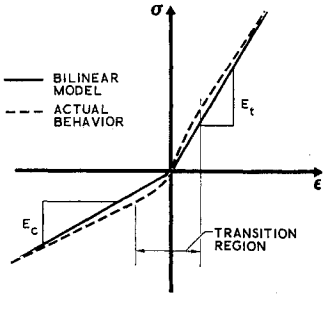

Fig. 2 Comparison of actual stress-strain behavior with the bilinear model.

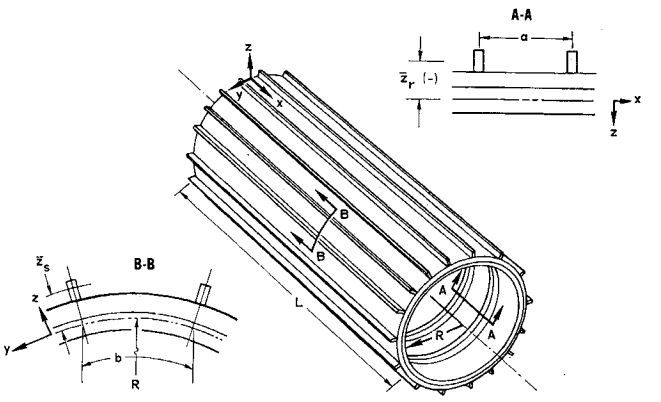

Fig. 3 Stiffened multilayered shell.

The logical steps necessary to determine the membrane prebuckling state are depicted schematically in Fig. 4. The first step is to make an arbitrary initial choice of the layer and stiffener stress signs in order to start the procedure. For convenience, the initial choice is all negative signs to denote compressive stresses. The second step is to determine the compliances S_{11}^k and S_{22}^k for each layer from Eq. (2) according to the chosen stress signs. The third step is to select an initial value for the cross-compliance S_{12}^k (note that S_{12}^k cannot be determined explicitly since the weighting factors, k_x^k and k_y^k, depend on the layer stress *values* as well as their *signs*). The fourth step is to calculate the relative membrane strains (relative because only the *proportions* of axial and compressive loading are required, not the magnitudes) from the given loading and the chosen material properties. The relative membrane strains are calculated from

$$\bar{\epsilon}_x = [k_1(B_{22} + E_r A_r/a) - k_2 B_{12}]/[(B_{11} + E_s A_s/b)(B_{22} + E_r A_r/a) - B_{12}^2] \quad (9a)$$

$$\bar{\epsilon}_y = [k_2(B_{11} + E_s A_s/b) - k_1 B_{12}]/[(B_{11} + E_s A_s/b)(B_{22} + E_r A_r/a) - B_{12}^2] \quad (9b)$$

which are obtained by inversion of the force-strain relations

$$\bar{N}_x = (B_{11} + E_s A_s/b)\epsilon_x + B_{12}\epsilon_y \quad (10a)$$

$$\bar{N}_y = B_{12}\epsilon_y + (B_{22} + E_r A_r/a)\epsilon_y \quad (10b)$$

and further redefinition of the loading as

$$\bar{N}_x = k_1\lambda \qquad \bar{N}_y = k_2\lambda \quad (11)$$

where λ is a measure of the magnitude of the loading and is

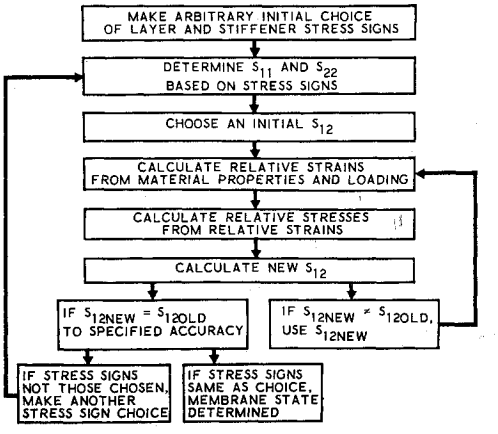

Fig. 4 Logic for determination of membrane prebuckling state.

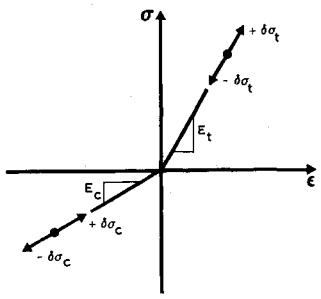

Fig. 5 Variations of stresses for a material with different moduli in tension and compression.

used to normalize the actual strains to obtain the relative strains. In Eq. (9), the B_{ij} are the extensional stiffnesses of the layered shell defined later in Eq. (23). The fifth step is to calculate the relative layer stresses from the relative strains by use of Eq. (6). The sixth step is to recalculate the cross-compliance $S_{12}{}^k$ now that the relative magnitudes of the layer stresses are available to determine the weighting factors, $k_x{}^k$ and $k_y{}^k$. The seventh step is to compare the newly calculated $S_{12}{}^k$ with the previous value. If the two $S_{12}{}^k$ do not agree to within a specified accuracy, then the new $S_{12}{}^k$ is used in another iteration of steps four through seven until the value of $S_{12}{}^k$ consistent with the chosen stress signs is obtained. The eighth step is to compare the stress signs calculated by use of Eq. (6) with the chosen stress signs. If the two sets of signs agree, then a consistent membrane prebuckling state has been determined. Otherwise, another set of stress signs must be chosen and steps two through eight repeated.

Discussion of how to choose the next set of layer and stiffener stress signs is important because of the number of sets of possible stress signs. It is easily verified that for an N-layered shell with rings and stringers, the number of different combinations of stress signs is 4^{N+1}. For example, a single-layered shell has four combinations of signs of σ_x and σ_y. A two-layered shell has sixteen combinations. A ring-stiffened two-layered shell has 32 combinations (4^2 times 2) and so on, including a ten-layered shell with 1,048,576 possible combinations of stress signs (an entirely practical case to consider since laminated fiber-reinforced composite materials often have ten or more layers). Obviously, it is impossible to store all possible combinations of stress signs in a computer for ready reference to see if a particular combination has already been tested in the searching procedure outlined in the preceding paragraph. Two alternatives were investigated and are incorporated in the BOMS II computer program developed by the author.[11] The first alternative is to use the calculated stress signs from the ith search in the $i+1$th search. Generally this procedure has been infallible in the cases examined by the author. However, the possibility exists of an oscillation between two sets of stress signs that bear no relation to the actual answer. This possibility is accounted for in the BOMS II computer program by storing three successive sets of stress signs and checking for repetition. If oscillation occurs, or if the number of cases investigated exceeds an arbitrary number [say, $(4^{N+1})/4$], on the assumption that convergence will not be obtained, then the second procedure is undertaken. This second procedure is simply a systematic investigation of each of the possible combinations of layer and stiffener stress signs without repetition. The word systematic is appropriate since a binary number of length 4^{N+1} is established, each element of which represents the sign of a stress. The binary number is given initial value zero to denote all compressive stresses and 1 is added to generate each new possible set of stress signs. However, considerable time can be required to determine the correct set of stress signs since a large number of possible combinations must be investigated. For a ten-layered shell, the time required to examine all possible combinations is on the order of eight hours on an IBM 360/65 computer. Fortunately, the first procedure works for the problems investigated by the author and required only about 0.9 sec for a ten-layered shell.

Variations of Stresses and Strains during Buckling

During buckling, the stresses vary from their prebuckling values in the manner shown schematically in Fig. 5 where E_t and E_c denote the tensile and compressive values of any orthotropic modulus. There, the variations of stresses take place according to the sign of the pertinent stress and the corresponding modulus. Let the variation be denoted by δ, whereupon from Eq. (6),

$$\delta\sigma_x{}^k = K_{11}{}^k\delta\epsilon_x{}^k + K_{12}{}^k\delta\epsilon_y{}^k \tag{12a}$$

$$\delta\sigma_y{}^k = K_{12}{}^k\delta\epsilon_x{}^k + K_{22}{}^k\delta\epsilon_y{}^k \tag{12b}$$

$$\delta\tau_{xy}{}^k = K_{33}{}^k\delta\gamma_{xy}{}^k \tag{12c}$$

Note that the variation of Eq. (6) has been supplemented by a relation between the variations in shear stress and shear strain. Such a relation is required since, although the shear stress is zero in the (principal stress) x-y coordinates, the variation in shear stress during buckling is not zero. The quantity $K_{33}{}^k$ is actually the shear modulus of an orthotropic material in principal stress coordinates and is the inverse of the shear compliance $S_{33}{}^k$ which takes on the following values:

$$\text{if } \sigma_x{}^k > 0 \text{ and } \sigma_y{}^k > 0; \quad S_{33}{}^k = S_{33t}{}^k \tag{13a}$$

$$\text{if } \sigma_x{}^k < 0 \text{ and } \sigma_y{}^k < 0; \quad S_{33}{}^k = S_{33c}{}^k \tag{13b}$$

$$\text{if } \sigma_x{}^k > 0 \text{ and } \sigma_y{}^k < 0; \quad S_{33}{}^k = k_x{}^kS_{33t}{}^k + k_y{}^kS_{33c}{}^k \tag{13c}$$

$$\text{if } \sigma_x{}^k < 0 \text{ and } \sigma_y{}^k > 0; \quad S_{33}{}^k = k_x{}^kS_{33c}{}^k + k_y{}^kS_{33t}{}^k \tag{13d}$$

where $k_x{}^k$ and $k_y{}^k$ are defined in Eq. (5) and

$$S_{33}{}^k{}_t = \frac{1}{G_t{}^k} = \frac{4}{E_{45t}{}^k} - \left(\frac{1}{E_{xt}{}^k} + \frac{1}{E_{yt}{}^k} - \frac{2\nu_{xyt}{}^k}{E_{xt}{}^k}\right) \tag{14}$$

(with a similar expression defining $S_{33c}{}^k$). The quantity $E_{45t}{}^k$ is the tensile modulus at 45° to the x direction suggested by Tsai.[12] Such a quantity must be defined because the tensile and compressive shear moduli of an orthotropic material with different moduli in tension and compression cannot be measured in a shear test (a state of pure tension or pure compression is impossible, therefore an $S_{33t}{}^k$ or $S_{33c}{}^k$ cannot be measured directly, but must be inferred from other data). A shear modulus for such a material, when measured in a direct shear test, exhibits different values when the sign of the shear stress is reversed.

In accordance with the Kirchhoff-Love hypothesis, a linear strain distribution exists in the layered shell during buckling. Thus, the variations of strains in the kth layer during buckling are

$$\delta\epsilon_x{}^k = \delta\epsilon_1 + z_k\delta\chi_1 \tag{15a}$$

$$\delta\epsilon_y{}^k = \delta\epsilon_2 + z_k\delta\chi_2 \tag{15b}$$

$$\delta\gamma_{xy}{}^k = \delta\epsilon_3 + z_k\delta\chi_3 \tag{15c}$$

where z_k is the distance from the shell reference surface to a point in the kth layer. In Eq. (15), $\delta\epsilon_1$, $\delta\epsilon_2$, and $\delta\epsilon_3$ are the variations of the middle surface strains

$$\delta\epsilon_1 = \delta u_{,x} \tag{16a}$$

$$\delta\epsilon_2 = \delta v_{,y} + \delta w/R \tag{16b}$$

$$\delta\epsilon_3 = \delta u_{,y} + \delta v_{,x} \tag{16c}$$

and $\delta\chi_1$, $\delta\chi_2$, and $\delta\chi_3$ are the variations of the middle surface curvatures

$$\delta\chi_1 = -\delta w_{,xx} \tag{17a}$$

$$\delta\chi_2 = -\delta w_{,yy} \tag{17b}$$

$$\delta\chi_3 = -2\delta w_{,xy} \tag{17c}$$

Upon substitution of the variation of strains, Eq. (15), in the variations of stresses, Eq. (12),

$$\delta\sigma_x{}^k = K_{11}{}^k(\delta\epsilon_1 + z_k\delta\chi_1) + K_{12}{}^k(\delta\epsilon_2 + z_k\delta\chi_2) \tag{18a}$$

$$\delta\sigma_y{}^k = K_{12}{}^k(\delta\epsilon_1 + z_k\delta\chi_1) + K_{22}{}^k(\delta\epsilon_2 + z_k\delta\chi_2) \tag{18b}$$

$$\delta\tau_{xy}{}^k = K_{33}{}^k(\delta\epsilon_3 + z_k\delta\chi_3) \tag{18c}$$

Variations of Forces and Moments during Buckling

The variations of forces and moments during buckling are obtained by integration of the variations of stresses over the shell layers and stiffeners. The effect of the stiffeners on the variations of forces and moments is averaged or "smeared out" over the stiffener spacing;

$$\delta N_x = \sum_{k=1}^{N} \int_{t_k} \delta\sigma_x{}^k dz + \frac{1}{b}\int_{A_s} \delta\sigma_x dA_s \tag{19a}$$

$$\delta N_y = \sum_{k=1}^{N} \int_{t_k} \delta\sigma_y{}^k dz + \frac{1}{a}\int_{A_r} \delta\sigma_y dA_r \tag{19b}$$

$$\delta N_{xy} = \sum_{k=1}^{N} \int_{t_k} \delta\tau_{xy}{}^k dz \tag{19c}$$

$$\delta M_x = \sum_{k=1}^{N} \int_{t_k} \delta\sigma_x{}^k z dz + \frac{1}{b}\int_{A_s} \delta\sigma_x z dA_s \tag{20a}$$

$$\delta M_y = \sum_{k=1}^{N} \int_{t_k} \delta\sigma_y{}^k z dz + \frac{1}{a}\int_{A_r} \delta\sigma_y z dA_r \tag{20b}$$

$$\delta M_{xy} = -\sum_{k=1}^{N} \int_{t_k} \delta\tau_{xy}{}^k z dz - \frac{G_s J_s}{2b}\chi_3 \tag{20c}$$

$$\delta M_{yx} = \sum_{k=1}^{N} \int_{t_k} \delta\tau_{xy}{}^k z dz + \frac{G_r J_r}{2a}\chi_3 \tag{20d}$$

where t_k denotes the thickness of the kth layer and N is the number of layers. The variations of stresses for the stiffeners are based on uniaxial isotropic reductions of the orthotropic stress-strain relations. The integrations in Eqs. (19) and (20) yield

$$\delta N_x = (B_{11} + E_sA_s/b)\epsilon_1 + B_{12}\epsilon_2 + (C_{11} + \bar{z}_sE_sA_s/b)\chi_1 + C_{12}\chi_2 \tag{21a}$$

$$\delta N_y = B_{12}\epsilon_1 + (B_{22} + E_rA_r/a)\epsilon_2 + C_{12}\chi_1 + (C_{22} + \bar{z}_rE_rA_r/a)\chi_2 \tag{21b}$$

$$\delta N_{xy} = B_{33}\epsilon_3 + C_{33}\chi_3 \tag{21c}$$

$$\delta M_x = (C_{11} + \bar{z}_sE_sA_s/b)\epsilon_1 + C_{12}\epsilon_2 + (D_{11} + \bar{z}_s{}^2E_sA_s/b + E_sI_s/b)\chi_1 + D_{12}\chi_2 \tag{22a}$$

$$\delta M_y = C_{12}\epsilon_1 + (C_{22} + \bar{z}_rE_rA_r/a)\epsilon_2 + D_{12}\chi_1 + (D_{22} + \bar{z}_r{}^2E_rA_r/a + E_rI_r/a)\chi_2 \tag{22b}$$

$$\delta M_{xy} = -C_{33}\epsilon_2 - (D_{33} + G_sJ_s/2b)\chi_3 \tag{22c}$$

$$\delta M_{yx} = C_{33}\epsilon_3 + (D_{33} + G_rJ_r/2a)\chi_3 \tag{22d}$$

where

$$B_{ij} = \sum_{k=1}^{N} K_{ij}{}^k(\delta_k - \delta_{k-1}) \tag{23a}$$

$$C_{ij} = \frac{1}{2}\sum_{k=1}^{N} K_{ij}{}^k[(\delta_k{}^2 - \delta_{k-1}{}^2) - 2\Delta(\delta_k - \delta_{k-1})] \tag{23b}$$

$$D_{ij} = \frac{1}{3}\sum_{k=1}^{N} K_{ij}{}^k[(\delta_k{}^3 - \delta_{k-1}{}^3) - 3\Delta(\delta_k{}^2 - \delta_{k-1}{}^2) + 3\Delta^2(\delta_k - \delta_{k-1})] \tag{23c}$$

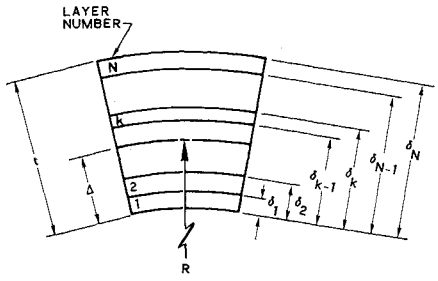

Fig. 6 Cross section of an N-layered shell.

in which N is the number of layers, δ_k is the distance from the inner surface of the layered shell to the outer surface of the kth layer, and Δ is the distance from the inner surface of the layered shell to the reference surface. The stiffnesses in Eq. (23) are due to Ambartsumyan[13] and depend on the location of the reference surface (see Fig. 6).

Stability Differential Equations

The Donnell-type stability differential equations for circular cylindrical shells subjected to arbitrary combinations of axial and lateral pressure are

$$\delta N_{x,x} + \delta N_{xy,y} = 0 \tag{24a}$$

$$\delta N_{xy,x} + \delta N_{y,y} = 0 \tag{24b}$$

$$-\delta M_{x,xx} + \delta M_{xy,xy} - \delta M_{yx,xy} - \delta M_{y,yy} + \delta N_y/R + \bar{N}_x\delta w_{,xx} + \bar{N}_y\delta w_{,yy} = 0 \tag{24c}$$

and the alternative force and geometric boundary conditions at $x = 0$ are chosen from the following sixteen possibilities (any set of four alternatives in the following pairs constitutes an acceptable set of boundary conditions):

$$\delta N_x = 0 \text{ or } \delta u = 0 \tag{25a}$$

$$\delta N_{xy} = 0 \text{ or } \delta v = 0 \tag{25b}$$

$$\delta M_{x,x} + \delta M_{yx,y} + \bar{N}_x\delta w_{,x} = 0 \text{ or } \delta w = 0 \tag{25c}$$

$$\delta M_x = 0 \text{ or } \delta w_{,x} = 0 \tag{25d}$$

Upon substitution of the expressions for the variations of forces and moments during buckling [Eqs. (21) and (22)] and the variations of reference surface strains and changes of curvature [Eqs. (16) and (17)], the stability differential equations become,

$$(B_{11} + E_sA_s/b)\delta u_{,xx} + B_{12}(\delta v_{,xy} + \delta w_{,x}/R) + B_{33}(\delta u_{,yy} + \delta v_{,xy}) - (C_{11} + \bar{z}_sE_sA_s/b)\delta w_{,xxx} - (C_{12} + 2C_{33})\delta w_{,xyy} = 0 \tag{26a}$$

$$B_{12}\delta u_{,xy} + (B_{22} + E_rA_r/a)(\delta v_{,yy} + \delta w_{,y}/R) + B_{33}(\delta u_{,xy} + \delta v_{,xx}) - (C_{12} + 2C_{33})\delta w_{,xxy} - (C_{22} + \bar{z}_rE_rA_r/a)\delta w_{,yyy} = 0 \tag{26b}$$

$$(B_{12}/R)\delta u_{,x} - (C_{11} + \bar{z}_sE_sA_s/b)\delta u_{,xxx} - (C_{12} + 2C_{33}) \times (\delta u_{,xyy} + \delta v_{,xxy}) + (1/R)(B_{22} + E_rA_r/a) \times (\delta v_{,y} + \delta w/R) + (C_{22} + \bar{z}_rE_rA_r/a)\delta v_{,yyy} - (2C_{12}/R)\delta w_{,xx} + (2/R)(C_{22} + \bar{z}_rE_rA_r/a)\delta w_{,yy} + (D_{11} + \bar{z}_s{}^2E_sA_s/b + E_sI_s/b)\delta w_{,xxxx} + (4D_{33} + 2D_{12} + G_sJ_s/b + G_rJ_r/a)\delta w_{,xxyy} + (D_{22} + \bar{z}_r{}^2E_rA_r/a + E_rI_r/a)\delta w_{,yyyy} + \bar{N}_x\delta w_{,xx} + \bar{N}_y\delta w_{,yy} = 0 \tag{26c}$$

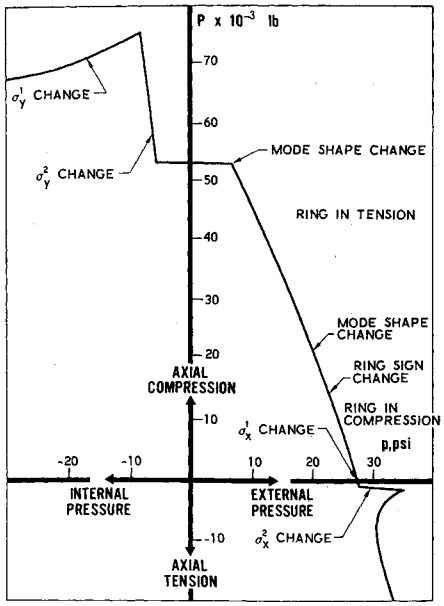

Fig. 7 Buckling of a ring-stiffened two-layered shell.

Buckling Criterion

It is desired to find the solution to the stability differential equations for the particular simply supported edge boundary conditions

$$\delta N_x = \delta v = \delta w = \delta M_x = 0 \tag{27}$$

The following buckling displacements satisfy the boundary conditions of Eq. (27):

$$\delta u = \bar{u} \cos(m\pi x/L) \sin(ny/R) \tag{28a}$$

$$\delta v = \bar{v} \sin(m\pi x/L) \sin(ny/R) \tag{28b}$$

$$\delta w = \bar{w} \sin(m\pi x/L) \cos(ny/R) \tag{28c}$$

(where $\bar{u}$, $\bar{v}$, and $\bar{w}$ are the amplitudes of the indeterminate buckling displacements) and are substituted in the stability differential equations, Eq. (26), to yield homogeneous equations in $\bar{u}$, $\bar{v}$, and $\bar{w}$. In order to obtain a nontrivial solution to the homogeneous equations, i.e., an exact solution to the stability differential equations, the determinant of the coefficients of, $\bar{u}$, $\bar{v}$, and $\bar{w}$ must be zero, and the following buckling criterion results:

$$\bar{N}_x\left(\frac{m\pi}{L}\right)^2 + \bar{N}_y\left(\frac{n}{R}\right)^2 = A_{33} + A_{23}\left(\frac{A_{13}A_{12} - A_{11}A_{23}}{A_{11}A_{22} - A_{12}^2}\right) + A_{13}\left(\frac{A_{12}A_{23} - A_{13}A_{22}}{A_{11}A_{22} - A_{12}^2}\right) \tag{29}$$

where

$$A_{11} = (B_{11} + E_sA_s/b)(m\pi/L)^2 + B_{33}(n/R)^2 \tag{30a}$$

$$A_{12} = (B_{12} + B_{33})(m\pi/L)(n/R) \tag{30b}$$

$$A_{13} = (B_{12}/R)(m\pi/L) + (C_{11} + \bar{z}_sE_sA_s/b)(m\pi/L)^3 + (C_{12} + 2C_{33})(m\pi/L)(n/R)^2 \tag{30c}$$

$$A_{22} = B_{33}(m\pi/L)^2 + (B_{22} + E_rA_r/a)(n/R)^2 \tag{30d}$$

$$A_{23} = (C_{12} + 2C_{33})(m\pi/L)^2(n/R) + (1/R)(B_{22} + E_rA_r/a)(n/R) + (C_{22} + \bar{z}_rE_rA_r/a)(n/R)^3 \tag{30e}$$

$$A_{33} = (D_{11} + E_sI_s/b + \bar{z}_s^2E_sA_s/b)(m\pi/L)^4 + (4D_{33} + 2D_{12} + G_sJ_s/b + G_rJ_r/a)(m\pi/L)^2(n/R)^2 + (D_{22} + E_rI_r/a + \bar{z}_r^2E_rA_r/a)(n/R)^4 + (2C_{12}/R) \times (m\pi/L)^2 + (2/R)(C_{22} + \bar{z}_rE_rA_r/a)(n/R)^2 + (1/R)^2(B_{22} + E_rA_r/a) \tag{30f}$$

The solution represented by Eq. (29) reduces to the solution of Jones[8] for eccentrically stiffened circular cylindrical shells with multiple orthotropic layers and to the solution of Jones[9] for circular cylindrical shells with a single isotropic layer having different moduli in tension and compression.

The applied in-plane forces, $\bar{N}_x$ and $\bar{N}_y$, can be related to a positive number λ according to

$$\bar{N}_x = k_1\lambda \qquad \bar{N}_y = k_2\lambda \tag{31}$$

Then, the left-hand side of Eq. (29) can be written as

$$\bar{N}_x(m\pi/L)^2 + \bar{N}_y(n/R)^2 = \lambda[k_1(m\pi/L)^2 + k_2(n/R)^2] \tag{32}$$

The special cases of axial compression, lateral pressure, and hydrostatic pressure are obtained with $k_1 = -1, k_2 = 0$; $k_1 = 0$, $k_2 = -1$; and $k_1 = -\frac{1}{2}$, $k_2 = -1$, respectively. More general cases of biaxial loading are obtained by specifying other values of k_1 and k_2, including cases wherein k_1 and/or k_2 are positive (tension).

The buckling load calculated from Eq. (29) depends on the geometry, material properties, and buckling mode parameters m and n. To find the minimum buckling load for a specified range of discrete values of m and n, the minimization procedure described by Jones[14] is used. Because of the numerous repetitive calculations in the minimization procedure, the many variables in Eq. (29), and the need for iteration to resolve the indeterminancy of the membrane prebuckled state, a computer program is essential to the practical calculation of buckling loads.[11]

Numerical Example

Because of the many geometrical and material parameters in the buckling criterion, meaningful general results cannot be presented. Accordingly, a specific numerical example is given to illustrate application of the buckling criterion to a previously insolvable problem.

In this example, a study is presented of the buckling of a ring-stiffened circular cylindrical shell (R = 6 in. and L = 12 in.) with an orthotropic outer layer (t_2 = 0.040 in.) that has different moduli in tension and compression and an isotropic inner layer (t_1 = 0.020 in.). The orthotropic layer properties are contrived to exhibit some of the general characteristics of current laminated glass fiber-reinforced phenolic materials:

$$E_{xt} = 2 \times 10^6 \text{ psi} \quad E_{yt} = 4 \times 10^6 \text{ psi}$$

$$\nu_{xyt} = 0.2 \quad E_t' = 2.5 \times 10^6 \text{ psi}$$

$$E_{xc} = 1 \times 10^6 \text{ psi} \quad E_{yc} = 2 \times 10^6 \text{ psi}$$

$$\nu_{xyc} = 0.3 \quad E_c' = 1.25 \times 10^6 \text{ psi}$$

However, it must be recognized that the current available data is not extensive enough nor definitive enough to imply the specific material properties displayed. The shear stiffnesses implied by the given properties are quite low as is typical of fiber-reinforced composites. The isotropic layer is aluminum with $E = 10 \times 10^6$ psi and $\nu = 0.3$. The rings of rectangular cross section (height = 0.05 in. and width = 0.04 in.) are aluminum with the same material properties as the inner layer to which they are fastened at a 1-in. spacing.

The buckling behavior of the example shell is shown on the biaxial loading plot in Fig. 7. There, discontinuities in buckling load occur where the sign of the stress in the second (orthotropic) layer changes since the modulus changes radically. These discontinuities are analogous to the discontinuities observed for single-layered shells by the author[9] when a component of the loading changes sign. The discontinuities in buckling load occur because of the discontinuity in slope of the stress-strain curve typified by Fig. 1. For nonlinear transition from E_t to E_c, the discontinuities would not exist, but the shape of the biaxial buckling curve would be smoothed out (and be much harder to obtain because of the nonlinearity introduced in the problem). Note that

the discontinuities in buckling load occur along a line P/p = constant, i.e., the ratio of applied forces is the determining factor in the calculation of the buckling loads. Note also that the rings are in tension for much of the biaxial loading range shown.

The buckling load discontinuity seems more pronounced for near-axial compression loading than for near-lateral pressure loading. This observation can be rationalized by examination of the following approximate expressions for buckling of long circular cylindrical shells under lateral pressure p and axial compression P, respectively:

$$\bar{p} = (5.51/LR^{3/2})(1 - \nu_{xyB}\nu_{yxB})^{1/4}B_{11}{}^{1/4}D_{22}{}^{3/4} \quad (33)$$

$$\bar{P} = (2/R)(1 - \nu_{xyB}\nu_{yxB})^{1/2}B_{22}{}^{1/2}D_{11}{}^{1/2} \quad (34)$$

wherein ν_{xyB} and ν_{yxB} are Poisson's ratios for extension of the multilayered shell. For lateral pressure, the axial extensional stiffness, B_{11}, has much less importance in the buckling calculation than the circumferential bending stiffness, D_{22}, because B_{11} occurs in Eq. (33) to a much lower power than D_{22}. Similarly, for axial compression, the circumferential extensional stiffness, B_{22}, has about the same importance in the buckling calculation as does the axial bending stiffness, D_{11}. Thus, from Eqs. (33) and (34), it is apparent that the modulus in the direction normal to the principal loading has a greater effect for axial compression than for lateral pressure.

Other combinations of geometry and material properties result in buckling load discontinuities in more profusion and at other locations in a biaxial loading plot such as Fig. 7. For example, the discontinuities can occur on either or both sides of the zero axial load or zero lateral pressure lines.[11]

Concluding Remarks

An exact buckling criterion, within the framework of classical buckling theory, is derived for eccentrically stiffened multilayered circular cylindrical shells with different orthotropic moduli in tension and compression, a feature common to many current composite materials. The buckling criterion is valid for arbitrary combinations of axial and circumferential loading. The combinations include axial compression and internal pressure as well as axial tension and external pressure. The material model (stress-strain relationship) involves a bilinear stress-strain curve that has a discontinuity in slope (modulus) at the origin. Classical buckling theory, by which is implied a membrane prebuckled shape, is used for a set of simply supported edge boundary conditions.

The numerous geometrical and material parameters in the present investigation cannot be nondimensionalized in a meaningful fashion, i.e., general results cannot be presented. Accordingly, a numerical example for buckling of a ring-stiffened two-layered shell is given to illustrate application of the buckling criterion. Discontinuities in buckling loads are observed as the axial and circumferential loading change relative to one another. The discontinuities were observed by Jones[9] and are an inherent feature of the discontinuity in the stress-strain curve. The present results should serve as a guide to the conduct of experiments designed to study buckling of shells made of composite materials that exhibit different moduli in tension and compression.

References

[1] Ambartsumyan, S. A., "Specific Peculiarities of a Theory of Shells from Modern Materials," *Izvestiya akademii nauk armianskoi SSR, Mekhanika*, Vol. 21, No. 4, 1968, pp. 3–19; translation N69-27721, STAR.

[2] Babel, H. W., private communication, Feb. 1969, McDonnell/Douglas Astronautics Co., Western Div., Santa Monica, Calif.

[3] Ambartsumyan, S. A., "The Axisymmetric Problem of a Circular Cylindrical Shell Made of Material with Different Stiffness in Tension and Compression," *Izvestiya akademii nauk SSSR, Mekhanika*, No. 4, 1965, pp. 77–85; translation N69-11070, STAR.

[4] Ambartsumyan, S. A. and Khachatryan, A. A., "Basic Equations in the Theory of Elasticity for Materials with Different Stiffness in Tension and Compression," *Inzhenernyi zhurnal, Mekhanika tverdogo tela*, No. 2, 1966, pp. 44–53; translation LRG-67-T-12, The Aerospace Corp., El Segundo, Calif.

[5] Ambartsumyan, S. A., "Equations of the Plane Problem of the Multimodulus Theory of Elasticity," *Izvestiya akademii nauk armianskoi SSR, Mekhanika*, Vol. 19, No. 2, 1966, pp. 3–19; translation LRG-67-T-14, The Aerospace Corp., El Segundo, Calif.

[6] Ambartsumyan, S. A. and Khachatryan, A. A., "Theory of Multimodulus Elasticity," *Inzhenernyi zhurnal, Mekhanika tverdogo tela*, No. 6, 1966, pp. 64–67; translation N67-27610, STAR.

[7] Ambartsumyan, S. A., "Basic Equations and Relations in the Theory of Elasticity of Anisotropic Bodies with Differing Moduli in Tension and Compression," *Inzhenernyi zhurnal, Mekhanika tverdogo tela*, No. 3, 1969, pp. 51–61; translation LRG-70-T-1, The Aerospace Corp., El Segundo, Calif.

[8] Jones, R. M., "Buckling of Circular Cylindrical Shells with Multiple Orthotropic Layers and Eccentric Stiffeners," *AIAA Journal*, Vol. 6, No. 12, Dec. 1968, pp. 2301–2305; also "Errata," Vol. 7, No. 10, Oct. 1969, p. 2048.

[9] Jones, R. M., "Buckling of Circular Cylindrical Shells with Different Moduli in Tension and Compression," *AIAA Journal*, Vol. 9, No. 1, Jan. 1971, pp. 53–61.

[10] Block, D. L., Card, M. F., and Mikulas, M. M., Jr., *Buckling of Eccentrically Stiffened Orthotropic Cylinders*, TN D-2960, Aug. 1965, NASA.

[11] Jones, R. M., *BOMS II, Buckling of Stiffened Multilayered Circular Cylindrical Shells with Different Orthotropic Moduli in Tension and Compression*, The Aerospace Corporation TR-0059(S6825)-2, Aug. 1970, The Aerospace Corp., El Segundo, Calif. (available only from the Clearinghouse for Federal Scientific and Technical Information, U.S. Dept. of Commerce).

[12] Tsai, S. W., *A Test Method for the Determination of Shear Modulus and Shear Strength*, AFML-TR-66-372, Jan. 1967.

[13] Ambartsumyan, S. A., *Theory of Anisotropic Shells*, State Publishing House for Physical and Mathematical Literature, Moscow, 1961; also TT F-118, May 1964, NASA.

[14] Jones, R. M., "Plastic Buckling of Eccentrically Stiffened Multilayered Circular Cylindrical Shells," *AIAA Journal*, Vol. 8, No. 2, Feb. 1970, pp. 262–270.